Bulletin of the Seismological Society of America, Vol. 105, No. 1, pp. 167–176, February 2015, doi: 10.1785/0120140116

A Long-Term Seismic Quiescence before the 2004 Sumatra (M_w 9.1) Earthquake

by Kei Katsumata

Abstract The 2004 Sumatra (M_w 9.1) earthquake was preceded by a seismic quiescence that began 13 years before the mainshock. An earthquake catalog created by the International Seismological Centre is analyzed in the study area, 80°–110° E, 10° S–20° N, between 1964 and 2004, including 1153 earthquakes shallower than 100 km with body-wave magnitude of $5.0 \le m_b \le 6.7$. A detailed analysis of the earthquake catalog using a gridding technique (ZMAP) shows the quiescent area is located between 3° and 6° N, which covers the southeastern part of the focal area, including the rupture initiation point of the 2004 Sumatra earthquake. The observed spatial pattern of quiescence can be explained by stress perturbation due to a long-term slow slip located on the deeper edge of the mainshock fault, which is predicted by a numerical simulation based on a laboratory-derived friction law. Although the quiescence is not significant statistically, it may still be considered unlikely that such an anomalous quiescence would occur at almost the same time and location as other long-term anomalies reported in the previous studies, including decreases in *b*-value and tidal triggering.

Introduction

A giant earthquake occurred on 26 December 2004 in the Indian Ocean off the west coast of northern Sumatra, Indonesia (Fig. 1). The location of the hypocenter, determined by the U.S. Geological Survey (USGS), was 3.30° N, 95.98° E and 30 km in depth. According to the Global Centroid Moment Tensor (CMT) solution (Arvidsson and Ekström, 1998), the focal mechanism was a low-angle thrust type (strike = 329°, dip = 8°, and rake = 110°), and the seismic moment was $M_0 = 3.95 \times 10^{22}$ N·m (M_w 9.0); the USGS magnitude was M_w 9.1. This remarkable event was a typical subduction zone earthquake on the interface between the subducting Indo-Australian plate and the overriding Eurasian plate. The focal area ruptured by the 2004 Sumatra earthquake extended 1200–1300 km, from 2° to 14° N, along the Andaman trough (Ammon *et al.*, 2005; Tanioka *et al.*, 2006; Chlieh *et al.*, 2007; Tanioka and Gusman, 2012). It is noteworthy that the Global Positioning System network detected a clear precursory positive anomaly of ionospheric total electron content around the focal region several tens of minutes before the mainshock (Heki, 2011), as this type of anomaly is a controversial issue (e.g., Thomas *et al.*, 2012; Heki and Enomoto, 2013; Kamogawa and Kakinami, 2013).

Little is known of what is going on in the final stage of the earthquake occurrence cycle. One of the important clues to understanding the final stage is the seismicity rate change. Usually, small earthquakes occur in the interseismic period with a constant rate in subduction zones. According to the seismic quiescence hypothesis, when a great earthquake is impending, small earthquakes decrease in and around the area that will be ruptured by a subsequent mainshock (Mogi, 1969). Several cases support this hypothesis (e.g., Mogi, 1969; Ohtake *et al.*, 1977; Wyss, 1985). Wyss and Habermann (1988) summarized 17 cases of precursory seismic quiescence to mainshocks, with magnitudes ranging from **M** 4.7 to 8.0, and found that (1) the rate of decrease ranges from 45% to 90%, and (2) the duration of the precursors ranges from 15 to 75 months. Recently, more reliable precursory seismic quiescences have been reported: the 1988 Spitak earthquake (**M** 7.0; Wyss and Martirosyan, 1998), the 1992 Landers earthquake (**M** 7.5; Wiemer and Wyss, 1994), the 1994 Hokkaido-Toho-Oki earthquake (**M** 8.3; Katsumata and Kasahara, 1999), the 1995 Hyogo-ken Nanbu earthquake (**M** 7.3; Enescu and Ito, 2001), and the 2003 Tokachi-Oki earthquake (**M** 8.3; Katsumata, 2011a).

On the other hand, very few cases of seismic quiescences prior to giant (**M** 9 class) earthquakes are known. Kanamori (1981) pointed out that some giant earthquakes were preceded by seismic quiescences lasting more than 20 years. Katsumata (2011b) reported a long-term seismic quiescence that started 23.4 years before the 2011 Off the Pacific Coast of Tohoku earthquake (**M** 9.0). Imoto and Yamamoto (2008) detected seismicity rate increases two to four years prior to the 2004 Sumatra earthquake, and Bansal and Ogata (2013) found the seismic activation started in the middle of July 2000, about 4.5 years before the 2004 Sumatra earthquake. These two studies applied the epidemic-type aftershock sequence (ETAS) models to the seismicity, and thus a temporal change in

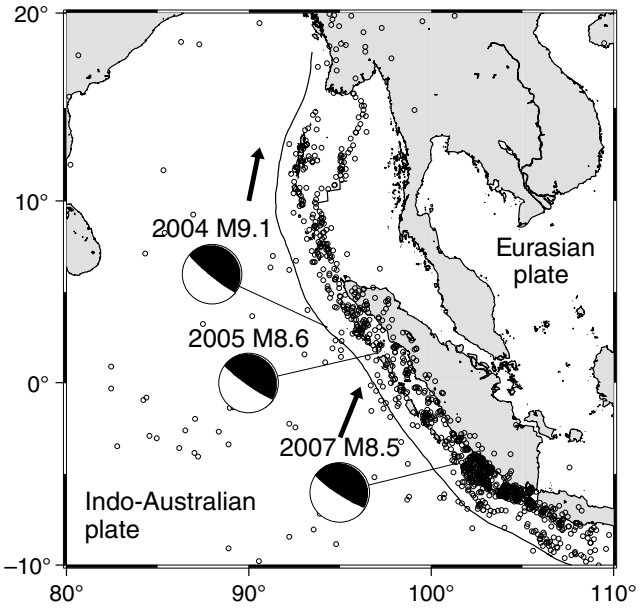

Figure 1. The study area along the Sumatra–Andaman subduction zone and the epicentral distribution of earthquakes used for calculating *Z*-values in this study (1 January 1964–25 December 2004, $5.0 \leq m_b \leq 6.7$, $0 \leq$ Depth[km] ≤ 100), which is the International Seismological Centre (ISC) earthquake catalog after a declustering process is applied. The focal mechanisms of great earthquakes equal to M_w 8.5 or larger, including the 2004 Sumatra, the 2005 Nias, and the 2007 Bengkulu earthquakes (which were determined by the Global Centroid Moment Tensor [CMT] project) are shown. The arrows indicate the direction of plate motion relative to the Eurasian plate (DeMets *et al.*, 1994).

seismicity was modeled appropriately and the statistical significance was estimated exactly. However, the spatial resolution was relatively poor, and consequently they might not be able to detect a long-term seismic quiescence. The purpose of this study is to identify and characterize a long-term change in seismicity rate (i.e., quiescence and/or activation) before the 2004 Sumatra earthquake with as much spatial and temporal resolution as possible.

Data

The International Seismological Centre (ISC) earthquake catalog for 1 January 1964 to 25 December 2004 is used. Various kinds of magnitude are reported in the ISC catalog, including body-wave magnitude m_b, surface wave magnitude M_s, moment magnitude M_w, and some local magnitudes. Body-wave magnitude m_b has been continuously determined and reported by ISC between 1964 and 2004. Reporting of surface wave magnitude M_s began in 1978. I use the earthquake list for m_b in this study. Earthquakes shallower than 100 km along the Andaman Islands, the Nicobar Islands, and the Great Sunda Islands are selected, including shallow earthquakes in the crust beneath the back-arc region.

The cumulative number of earthquakes versus magnitude for the catalog is checked to estimate the degree of magnitude completeness M_c using the method of Wiemer and Wyss (2000). As a result, M_c is ~5.0 from 1964 to 1970 and decreases gradually to 4.0 in 2004. Thus, I use earthquakes with $m_b \geq 5.0$, which are located, without fail, between 1964 and 2004. Because the m_b does not appropriately represent the size of large earthquakes, those with $5.0 \leq m_b \leq 6.7$ are used in this study.

Clustered events such as earthquake swarms and aftershocks are removed from the ISC catalog using a stochastic declustering method developed by Zhuang *et al.* (2002). The method divides seismicity into two processes based on the ETAS model: the background events and the clustered events. The background events are used in the following analysis. The nondeclustered original ISC catalog is compared with the background events catalog to check whether the method works well. The ISC catalog with body-wave magnitude band $5.0 \leq m_b \leq 6.7$ is declustered using this method. Although earthquakes larger than m_b 6.7 are not included, aftershocks following large earthquakes are removed rather effectively. For example, a great earthquake with **M** 7.8 on 4 June 2000 was followed by 27 aftershocks within one month in the aftershock area extending 100 km or more in the north–south direction. I confirmed that the aftershocks can clearly have been removed by using the stochastic declustering method.

Eventually, I use 1153 earthquakes selected from the ISC earthquake catalog in the $5.0 \leq m_b \leq 6.7$ range between 1964 and 2004, with depth shallower than 100 km and with applying the stochastic declustering method (Zhuang *et al.*, 2002), which is the basis of analysis of this study (Fig. 1).

Analysis

ZMAP

A simple gridding technique, ZMAP (Wiemer and Wyss, 1994), is used to systematically search the rate changes in space and time. Parameters for the ZMAP analysis are shown in Table 1. The grid size is $0.5° \times 0.5°$ in the study area (10° S–20° N, 80°–110° E). The epicentral distances are calculated for all pairs of earthquakes and the nodes, and I choose $N = 40$ earthquakes around each node. When selecting $N = 40$ events, a circle is drawn around each node, and its radius is increased until it includes a total of 40 epicenters. The parameter N is fixed for all nodes to allow statistical comparison. The largest epicentral distance among the $N = 40$ pairs defines the spatial resolution r for the node: r is small if the seismicity rate is high, and r is large if the seismicity rate is low. The 40 earthquakes selected occur in a time period between t_0 (1 January 1964) and t_e (25 December 2004). Based on the cumulative number curve for each node, the Z value is calculated as follows. First, I place a time window with a starting time of T_s and an ending time of $T_s + T_w$, assuming $T_w = 5$ years in this case. Second, the mean seismicity rate R_w in the time window T_w and the mean seismicity rate R_{bg} in the background time period are calculated. R_{bg} is defined in the time period between t_0 and t_e, excluding T_w. Then, the Z value is obtained by the following equation:

Table 1
Characteristic Parameters for ZMAP in This Study*

Parameter	Range or Value
Study area	80–110° E, 10° S–20° N
Start time of earthquake catalog	1 January 1964
End time of earthquake catalog	25 December 2004
Time length of earthquake catalog (days)	14,970
Body-wave magnitude range	$5.0 \le m_b \le 6.7$
Depth range of hypocenters (km)	0–100
The total number of earthquakes	1153
Grid interval	0.5° × 0.5°
Radius of resolution circles (km)	170
The number of effective grids	261
Length of bin (days)	28
Time step of T_s (years)	0.1
The number of time steps	359
The number of earthquakes for each grid	40
T_w (years)	5.0

*A cumulative number of $N = 40$ earthquakes as a function of time is the basis of the ZMAP analysis. The cumulative number plot starts at time t_0 (1 January 1964) and ends at time t_e (25 December 2004). A time window starts at T_s and ends at $T_s + T_w$, in which $t_0 \le T_s \le T_s + T_w \le t_e$.

$$Z = (R_{bg} - R_w)/(S_{bg}/n_{bg} + S_w/n_w)^{1/2},$$

in which S_{bg} and n_{bg} are the variance and number of samples in the background time period, respectively, and S_w and n_w are the variance and number of samples in the time window T_w, respectively. The Z value is calculated for all nodes in the study area at the starting time T_s, and the time window is advanced by steps of 0.1 years. Katsumata (2011a) also described the ZMAP method with a concrete example.

Figure 2 shows time slices of the Z-value maps for the ISC earthquake catalog between $T_s = 1975$ and 1999. The stochastic declustering process is applied before the calculation of the Z-values. For each time slice, all grid points in the study area are colored if the radius of resolution circle r is equal to 170 km or smaller, which is a definition of effective grid points. Each time slice has 261 effective grid points; and, because there are 359 time slices, the total number of grid points in which Z values are calculated is 93,699.

Seismic Quiescence

Among the 261 grid points, only six have Z-values equal to +6.6, which is the maximum Z-value in the time period $1964.1 < T_s < 1999.9$. Positive Z-values indicate the seismicity rate is lower than the background rate. The one grid point is located at (5.0° N, 94.5° E), which is referred to as anomaly 1. The other five grid points are located around (5.5° S, 105.5° E). Based on the location and starting time T_s, the latter five grid points are identified as one anomaly, which is referred to as anomaly 2.

The spatial extent of epicenters within the volume of anomaly 1 is shown in Figure 3. Most of the epicenters are concentrated between 4° and 6° N, where the rupture of the 2004 mainshock started and a large coseismic slip was observed. The cumulative number of earthquakes in the volume of anomaly 1 shows the seismic quiescence starts suddenly around the middle of 1991, and the seismicity rate decreases from 0.91 to 0.17 events per year (a drop of 81%). The quiescent period until 1999 is followed by a recovery of seismicity immediately before the mainshock. A similar temporal behavior is observed at a grid point (4.0° N, 96.5° E) near anomaly 1, which has a Z-value of +6.4 (Fig. 3).

The start time of anomaly 1 is 1991.7, obtained by calculating the $AS(t)$ function (Habermann, 1987; Wiemer and Wyss, 1994). The $AS(t)$ function quantitatively estimates the change point of the slope of the cumulative number curve. Thus, the seismic quiescence started 13.3 years before the mainshock ($2004.99 - 1991.7 = 13.3$ years). The spatial extent of the seismically quiescent area is defined by grid points with the Z-values equal to +6.4 or larger around anomaly 1 (Fig. 4). The epicentral distribution of earthquakes in the circles centered at these grid points indicates the area suffered from the seismic quiescence. Based on this definition, the seismically quiescent area extends 400 km northwestward from the southeastern end of the focal area ruptured by the 2004 Sumatra earthquake. The large coseismic slip was observed in the southeastern part of the ruptured area (Ammon *et al.*, 2005; Chlieh *et al.*, 2007; Tanioka and Gusman, 2012). This spatial match suggests the seismic quiescence has some relationship with the 2004 mainshock.

To confirm the spatial pattern, I download the hypocenter data relocated by a double-difference determination method (Pesicek *et al.*, 2010) and plot them on a vertical cross section (Fig. 4). The distribution of hypocenters going down toward the northeast is identified and is associated with the subduction of the Indo-Australia plate. The hypocenters in the quiescent area are located not only along the subducting plate deeper than 30 km but also in the crust beneath the land.

Statistical Significance of the Quiescence

A histogram of Z-values calculated at all the effective nodes indicates visually that few Z-values larger than +6.0 are observed in this case (Fig. 5). For example, the number of Z-values equal to or larger than +6.4 is 180, which is a very small fraction of 93,699. An alarm cube plot is another method of displaying Z-value anomalies that could be false alarms (Wiemer, 1996; Wyss *et al.*, 1996; Wyss and Martirosyan, 1998). In Figure 5, the horizontal axes indicate the spatial coordinates in the study area, and the vertical axis indicates time. "Positive anomaly" is defined as cases of $Z \ge +6.3$ at any node and any time between $T_s = 1964.1$ and 1999.9 for $N = 40$ and $T_w = 5$ years. Among them, the alarm cube includes only two outstanding positive anomalies, labeled as A1 and A2, which illustrate visually the anomaly with $Z = +6.6$ seems to be an unusual phenomenon in this region and in this time period.

Is $Z = +6.6$ really an unusual phenomenon? Even if we find a significant seismic quiescence by using a statistical parameter, this finding often is not real (Matthews and

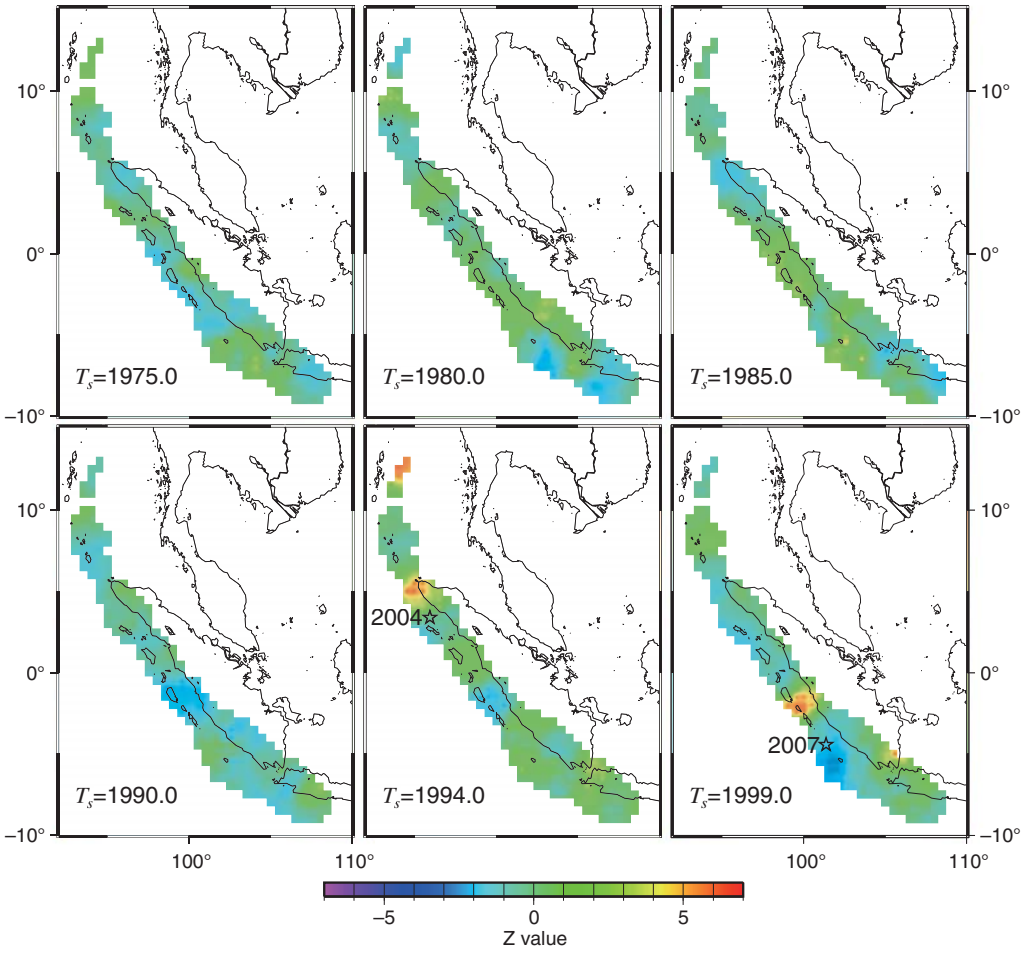

Figure 2. Time slices of Z-value distribution using the declustered ISC catalog. The time window starts at T_s and ends at $T_s + T_w$, in which $T_w = 5$ years. All grid points are colored if the radius of the resolution circle is smaller than 170 km. Red (positive Z-value) and blue (negative Z-value) represent a decrease and increase in the seismicity rate, respectively. Open stars in the time slices at $T_s = 1994.0$ and 1999.0 indicate the epicenters of the 2004 Sumatra and the 2007 Bengkulu earthquakes, respectively.

Reasenberg, 1988). To estimate the statistical significance of the Z-value anomaly detected in this study, a numerical simulation is conducted. First, a single date between 1 January 1964 and 25 December 2004 is extracted at random and repeated 1153 times to produce a synthetic earthquake catalog with 1153 earthquakes. Second, the extracted days are assigned to each earthquake; whereas the original values for both the longitude and the latitude of epicenter are retained. Because only time is shuffled, the distribution of seismicity is retained. Third, the Z-values are calculated in the same manner as mentioned above, and then the maximum Z-value (Z_{max}) is obtained. This procedure is repeated 2000 times, and Z_{max} is evaluated for each repetition.

As a result, all 2000 repetitions show $Z_{max} = +6.6$. This result means the $Z = +6.6$ anomaly is observed at least once somewhere in the time period between 1964 and 2004, even if the seismicity occurs at random. Therefore, the $Z = +6.6$ anomaly detected in this study is not a rare phenomenon. A seismic quiescence with $Z = +6.6$ is observed before the 2004 Sumatra earthquake in and around the southeastern end of the ruptured area; however, the abnormality has a high possibility of being an accidental coincidence.

USGS PDE Catalog

Bansal and Ogata (2013) compared two earthquake catalogs: the USGS Preliminary Determination of Epicenter (PDE) (National Earthquake Information Center) catalog and the ISC catalog; and they concluded the ISC catalog is not appropriate for investigating seismicity prior to the 2004 Sumatra earthquake. Here, I also compare the USGS and the ISC catalogs to show the results from the USGS catalog are almost the same as those from the ISC catalog. The USGS catalog used in this study includes earthquakes located in the area shown in Figure 1 between 1 January 1974 and 25 December 2004 with $\mathbf{M} \geq 5.0$, have depths shallower than 100 km, and for which a declustering process is not applied.

Epicenters in the volume of anomaly 1 are selected within the same radius of the resolution circle, that is, the same circular area as shown in Figure 3 and plotted in Figure 6. The start time of anomaly 1 is around the middle of 1991,

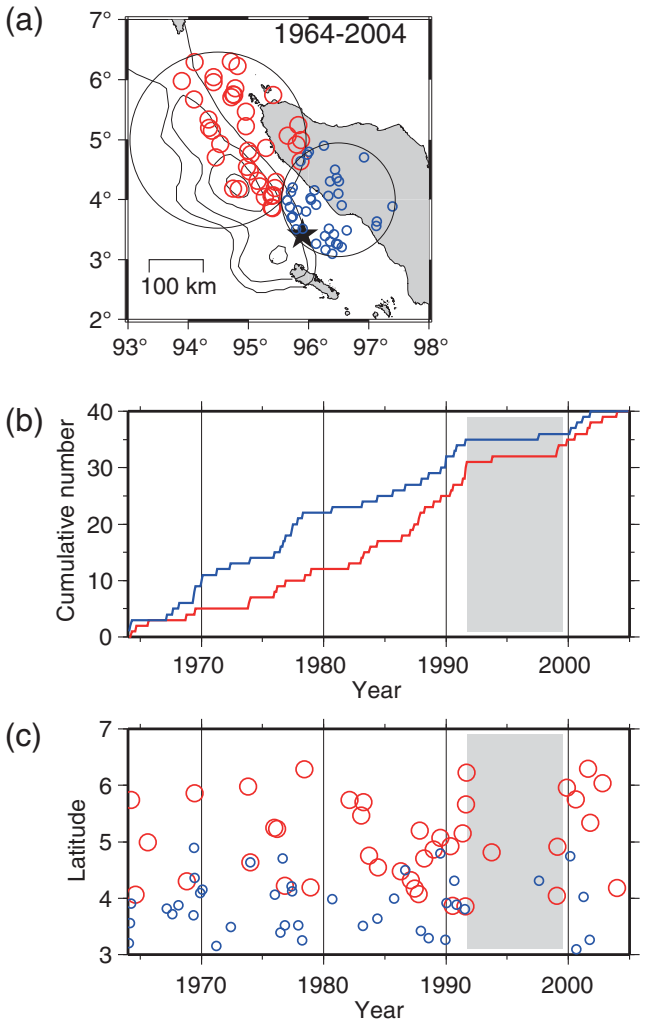

Figure 3. (a) The red and blue open circles are $N = 40$ epicenters sampled around the nodes with the Z-value anomalies of $Z = +6.6$ and $+6.4$, respectively, detected in Figure 2. The star indicates the epicenter of the 2004 Sumatra earthquake determined by the U.S. Geological Survey (USGS). A coseismic slip distribution model for the 2004 Sumatra earthquake is shown as contours every 5 m (Chlieh *et al.*, 2007). (b) Cumulative number curves for the sampled epicenters. The red and blue lines correspond respectively to the red and the blue epicenters in (a). (c) Space–time plots for the red and the blue epicenters in (a). Shaded areas in (b) and (c) indicate the time period of the seismic quiescence.

which is consistent with the start time obtained using the ISC catalog. The seismicity rate decreases from 2.1 to 1.1 events per year (a drop of 48%), which is consistent with the result from the ISC catalog, whereas the drop percentage is smaller.

As a conclusion, the agreement between the two catalogs confirms there is an apparent quiescence before the 2004 Sumatra earthquake in and around the southeastern part of the focal area. What remains to be resolved is whether this apparent quiescence results from a random fluctuation of the background seismicity rate or from a different mechanism.

Discussion

Comparison of the Observation with a Theory

According to the Global CMT solutions (Dziewonski *et al*, 1981), the down-dip-extension-type events occur deeper than 50 km in the quiescent area, suggesting that these are intraplate events within the subducting plate. Moreover in the quiescent area, the right-lateral strike-slip events are dominant shallower than 30 km beneath the land and are mainly associated with the seismicity along the Sumatra fault.

In the previous studies, some possible mechanisms have been proposed to explain the precursory seismic quiescence, including strain softening (Stuart, 1979), a bimodal distribution of fracture strength (Kanamori, 1981), and dilatancy hardening (Scholz, 1988). However, the most plausible model would be a regional stress relaxation due to preseismic sliding (Wyss *et al*, 1981; Kato *et al.*, 1997; Kato, 2003). Based on a numerical simulation, Kato *et al.* (1997) proposed a spatial pattern of precursory seismic quiescence. The intraplate compressional stress is expected to decrease within the overriding plate due to the preseismic quasistable sliding (fig. 10b in Kato *et al.*, 1997). In this study, I find the seismic quiescence within the overriding plate in and around the Sumatra fault. If the preseismic sliding is assumed to occur on the plate boundary around 30 km depth, the observed seismic quiescence is explained qualitatively. Although Kato *et al.* (1997) did not mention it explicitly, another change in seismicity is caused by the preseismic sliding. The compressional stress is expected to increase within the subducting plate around the deeper edge of the preseismic sliding. If the intermediate-depth seismicity within the subducting plate is caused by the down-dip tension (Simoes *et al*, 2004; Engdahl *et al.*, 2007), the seismicity rate should be suppressed. I find the down-dip-extensional-type events actually decrease within the subducting plate deeper than 30 km.

Duration Time of Quiescence

The duration of seismic quiescence T_q is defined as the time between the onset of quiescence and the mainshock. In this study, the duration is $T_q = 13.3$ years for the 2004 Sumatra earthquake (M_w 9.1). Many authors reported that some great earthquakes were preceded by a distinct long-term seismic quiescence. Here, I pick up the nine reliable recent results from the interplate subduction earthquakes: $T_q = 28$ years for the 1964 Alaska earthquake (M_w 9.2; Kanamori, 1981), $T_q = 21$ years for the 1957 Aleutian earthquake (M_w 9.1; Kanamori, 1981), $T_q = 23.4$ years for the 2011 Off the Pacific Coast of Tohoku earthquake (M_w 9.0; Katsumata, 2011b), $T_q = 5$ years for the 2003 Tokachi-Oki, Japan, earthquake (M_w 8.3; Katsumata, 2011a), $T_q = 6.3$ years for the 1968 Tokachi-Oki earthquake (M_w 8.2; Habermann, 1981), $T_q = 3.5$ years for the 1986 Aleutian earthquake (M_w 8.0; Kisslinger, 1988), $T_q = 5.3$ years for the 1976 Kermadec earthquake (M_w 7.9; Wyss *et al.*, 1984), $T_q = 5.5$ years for the 1978 Oaxaca earthquake (M_w 7.7;

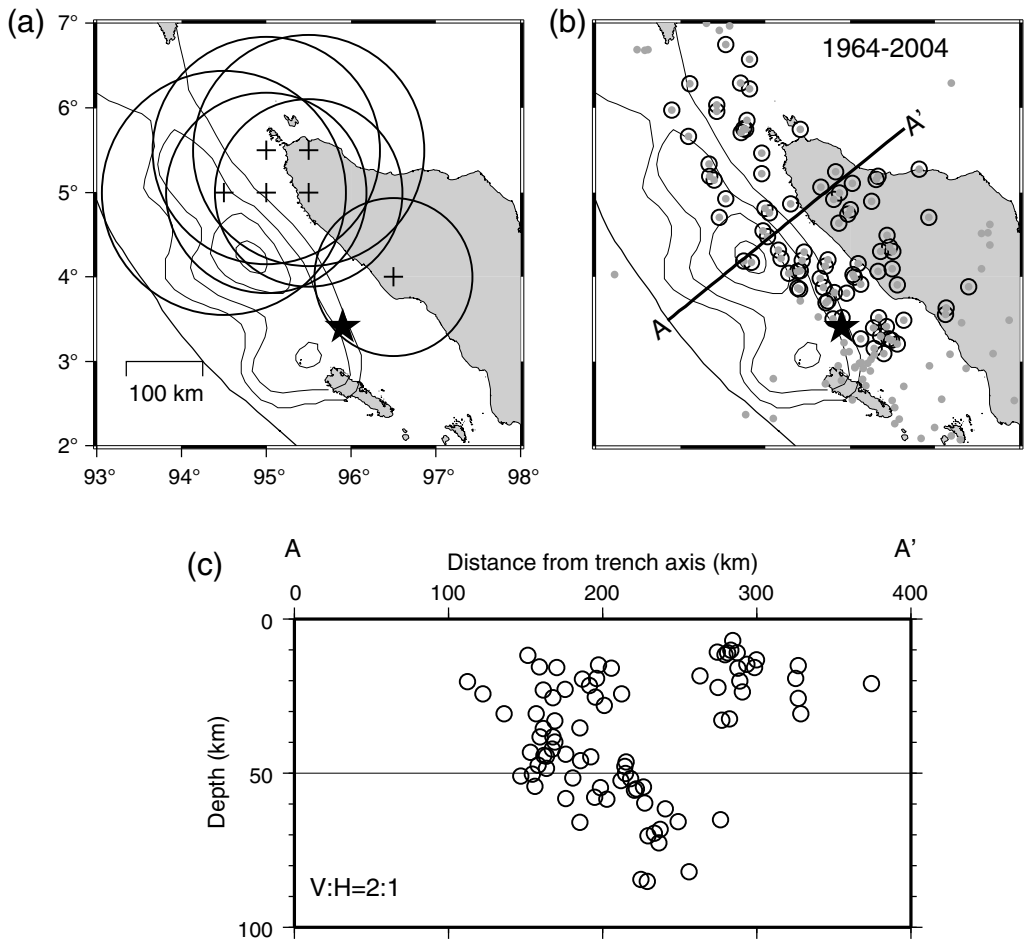

Figure 4. The spatial extent of the seismically quiescent area. (a) Crosses indicate nodes with the Z-value equal to +6.4 or larger, which are located spatiotemporally closely to the node at 5.0° N, 94.5° E, with the largest Z value of +6.6. Their resolution circles are also drawn. The star indicates the epicenter of the 2004 Sumatra earthquake determined by USGS. A coseismic slip distribution model for the 2004 Sumatra earthquake is shown with thin lines as contours every 5 m (Chlieh *et al.*, 2007). A bold line offshore indicates the trench axis. (b) Gray dots indicate the epicenters of earthquakes used in this study. Among them, the gray dots with black circles indicate the epicenters of earthquakes within the resolution circles in (a). (c) The vertical cross section along A–A′ in (b). All hypocenters plotted in (b) and (c) were relocated by Pesicek *et al.* (2010) using a double-difference seismic tomography method.

Ohtake *et al.*, 1977), and $T_q = 2.5$ years for the 1989 off Sanriku earthquake (M_w 7.4; Wyss *et al.*, 1999).

In fact, the duration of the apparent quiescence detected in this study is not 13.3 years long. The seismicity returns to close to its long-term rate in the late 1990s, as can be seen in Figure 3c and in the 1999 panel in Figure 2. This approximately five-year temporal gap between the end of the apparent quiescence and the mainshock is referred to as the β stage (Ohtake *et al.*, 1981). Such a renewal of seismicity was found for 28 cases among the 81 seismic quiescences (Ohtake, 1980). The physical mechanism of the β stage is not explained by the preseismic sliding model.

Additional Long-Term Changes

Nanjo *et al.* (2012) found the b-values began falling below $b = 1.2$ in 1988 in the southern part of the focal area of the 2004 Sumatra earthquake. The area and the start time of the b-value anomaly are consistent with those of the seismic quiescence observed in this study.

Tanaka (2010) observed tidal triggering of earthquakes before the 2004 Sumatra earthquake. She measured the correlation between the Earth's tide and earthquake occurrence in and around the focal region of the 2004 Sumatra earthquake. Statistical analysis indicated that a high correlation was observed for 10 years preceding the 2004 mainshock. Moreover, she found the precursory strong tidal correlation concentrated in the area around the rupture nucleation zone rather than in the northern part of the focal area. This fact suggests that earthquakes had been sensitive to tidal triggering in the seismically quiescent area prior to the mainshock.

Mignan *et al.* (2006) identified accelerating moment release (AMR) for the segments (5, 6, 7, and 8 in fig. 4 of Mignan *et al.*, 2006) with large coseismic slip of the 2004 Sumatra earthquake. However, Hardebeck *et al.* (2008) pointed out the AMR hypothesis is statistically insignificant.

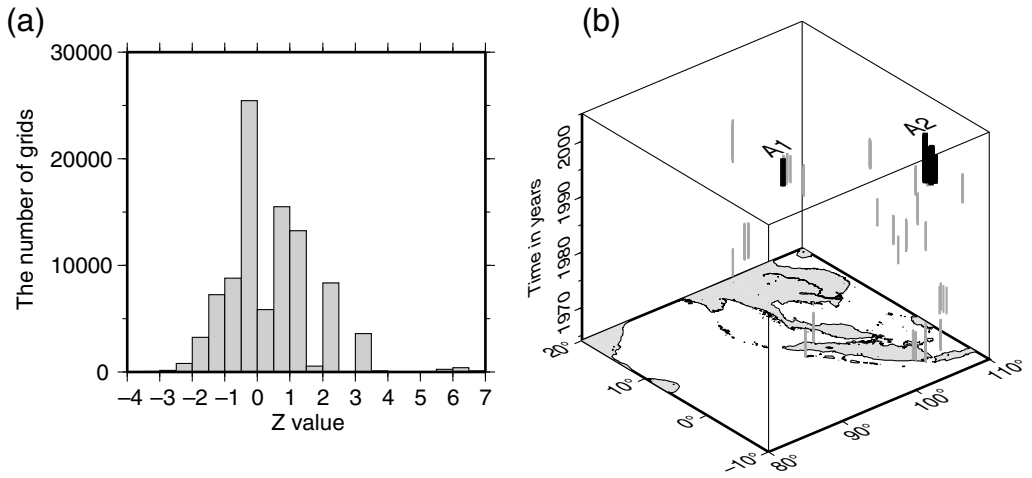

Figure 5. (a) Z-value distribution. The number of grid points in the study area is 3721 with a spacing of 0.5° × 0.5°; among them, the 261 grid points with a resolution circle equal to 170 km or smaller are selected for each time slice. Because there are 359 time slices from 1964.1 to 1999.9 with a time step of 0.1 years, the total number of grid points where Z-values are calculated is 93,699. (b) Alarm cube. The horizontal axes indicate the spatial coordinates in the study area, and the vertical axis indicates time. A positive anomaly is defined as cases of $Z \geq +6.3$ at any node and any time between $T_s = 1964.1$ and 1999.9 for $N = 40$ and $T_w = 5$ years. The bold lines labeled as A1 and A2 are the anomalies with $Z = +6.6$, which is the largest Z-value observed in this study.

Imoto and Yamamoto (2008) detected seismicity rate increases two to four years prior to the 2004 Sumatra earthquake, and Bansal and Ogata (2013) found the seismic activation started in the middle of July 2000, about 4.5 years before the 2004 Sumatra earthquake. These previous findings are consistent with the renewal of the seismicity rate following the quiescent period in the volume of anomaly 1, as mentioned in the Duration Time of Quiescence section.

False Alarm and Surprise Occurrence

The false alarm rate is defined as how often the seismic quiescence occurs without being closely followed by a mainshock. The surprise occurrence rate is defined as how often mainshocks occur that are not preceded by the seismic quiescence. Anomaly 2 in this study has not yet been followed by any mainshock, therefore this is a candidate for false alarm. On the other hand, in the Mentawai Islands region, a great earthquake with M_w 8.5 occurred on 12 September 2007 (Fig. 1), which is referred to as the 2007 Bengkulu earthquake in this study. The focal area was 250 × 100 km^2, and this event was a typical interplate earthquake similar to the 2004 Sumatra earthquake (Gusman *et al.*, 2010).

The 2007 Bengkulu earthquake is probably a case of surprise occurrence. In this study, a seismic quiescence is also identified prior to the 2007 Bengkulu earthquake (Fig. 7). However, the earthquakes within the quiescence volume are located far from the northern end of the focal area ruptured by the 2007 Bengkulu earthquake. The seismic quiescence starts in the middle of 1997 and lasts for about five years. In the period of the quiescence, no earthquake was observed, and the Z-value is +6.3. The $Z = +6.3$ anomaly is frequently observed, as shown in Figure 5, and thus it is not significant statistically. Therefore, I cannot conclude that this quiescence with $Z = +6.3$ has some relationship with the 2007 Bengkulu earthquake.

Conclusions

I investigate change in seismicity before the 2004 Sumatra (M_w 9.1) earthquake and find a long-term anomaly in seismic quiescence with duration time of 13.3 years. The degree of seismic quiescence is measured by Z-value as +6.6, and the area that suffered from this quiescence is located at the southeastern part of the focal area ruptured by the 2004 mainshock. Whereas, the quiescence with $Z = +6.6$ is not rare phenomenon, it may still be considered unlikely that such an anomaly would occur at almost the same time and location with other long-term anomalies reported in the previous studies, including decrease in b-value and tidal triggering. This fact might suggest an intermediate-term (several tens of years) precursory process definitely exists before a giant earthquake.

Data and Resources

The Sumatra Project database was searched using faculty.smu.edu/hdeshon/SUMATRA/index.html (last accessed March 2014). The Global Centroid Moment Tensor Project database was searched using www.globalcmt.org/ (last accessed March 2014). The Nagoya University (NGY) Seismological Notes was searched using www.seis.nagoya-u.ac.jp/sanchu/Seismo_Note/ (last accessed March 2014). The Earthquake Information Center Seismological Note was searched using http://wwweic.eri.u-tokyo.ac.jp/sanchu/Seismo_Note/ (last accessed March 2014).

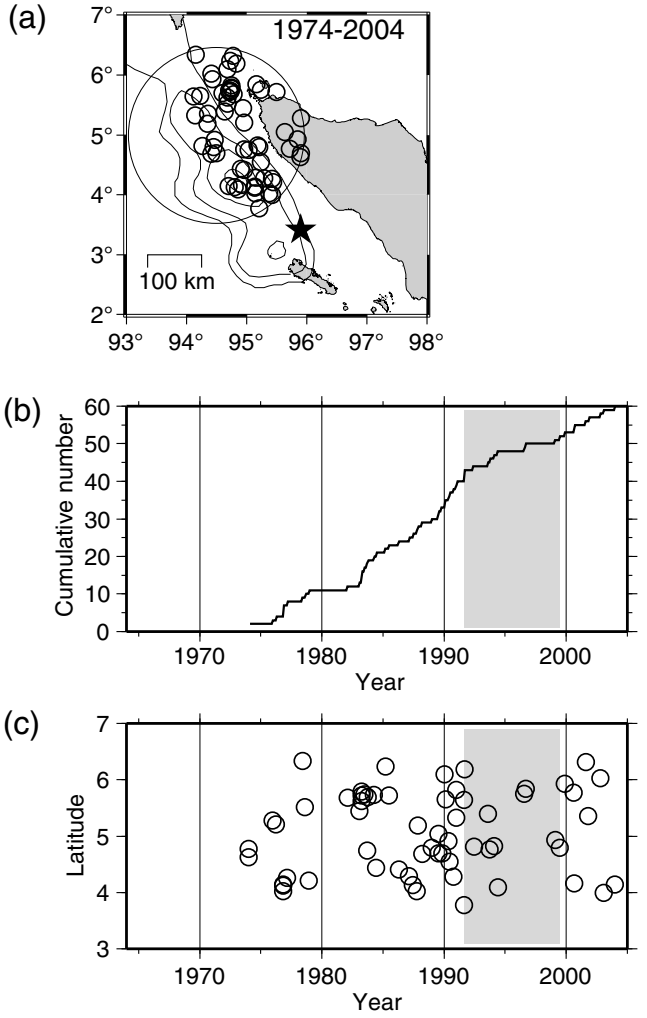

Figure 6. (a) Open circles are epicenters sampled around the nodes for anomaly 1. The USGS earthquake catalog is used between 1 January 1974 and 25 December 2004 with $\mathbf{M} \geq 5.0$, the depths are shallower than 100 km, and a declustering process is not applied. The radius of the circle for sampling earthquakes is the same as that in Figure 3. The star indicates the epicenter of the 2004 Sumatra earthquake determined by USGS. A coseismic slip distribution model for the 2004 Sumatra earthquake is shown as contours every 5 m (Chlieh *et al.*, 2007). (b) Cumulative number curves for the sampled epicenters. (c) Space–time plots for the epicenters in (a). Shaded areas in (b) and (c) indicate the time period of the seismic quiescence, which is the same as those in Figure 3.

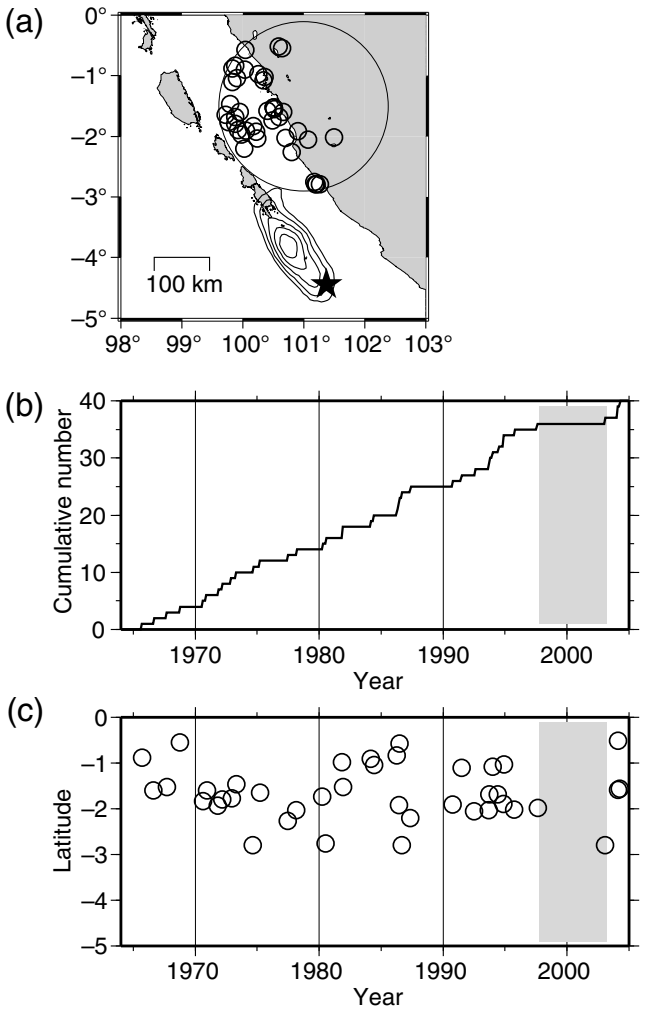

Figure 7. (a) Open circles are $N = 40$ epicenters sampled around the node with the Z-value of $Z = +6.3$. The star indicates the epicenter of the 2007 Bengkulu earthquake determined by USGS. A coseismic slip distribution model for the 2007 Bengkulu earthquake is shown as contours (*The NGY Seismological Notes*; see Data and Resources). (b) Cumulative number curves for the sampled epicenters. (c) Space–time plots for the epicenters in (a). The shaded areas in (b) and (c) indicate the time period of the seismic quiescence.

Acknowledgments

I thank S. Wiemer for providing the ZMAP software and H. Aoyama for helping revise the manuscript. The Generic Mapping Tools System (Wessel and Smith, 1991) is used to produce figures. I also thank J. L. Hardebeck and D. D. Fitzenz for valuable comments. This study was supported by the Ministry of Education, Culture, Sports, Science and Technology of Japan, under its Earthquake and Volcano Hazards Observation and Research Program.

References

Ammon, C. J., J. Chen, T. Hong-Kie, D. Robinson, N. Sidao, V. Hjorleifsdottir, H. Kanamori, T. Lay, S. Das, D. Helmberger, G. Ichinose, J. Polet, and D. Wald (2005). Rupture process of the 2004 Sumatra–Andaman earthquake, *Science* **308,** 1133–1139, doi: 10.1126/science.1112260.

Arvidsson, R., and G. Ekström (1998). Global CMT analysis of moderate earthquakes, $M_w \geq 4.5$, using intermediate period surface waves, *Bull. Seismol. Soc. Am.* **88,** 1003–1013.

Bansal, A. R., and Y. Ogata (2013). A non-stationary epidemic type aftershock sequence model for seismicity prior to the December 26, 2004 M 9.1 Sumatra–Andaman Islands mega-earthquake, *J. Geophys. Res.* **118,** 616–629, doi: 10.1002/jgrb.50068.

Chlieh, M., J. Avouac, V. Hjorleifsdottir, T. Song, C. Ji, K. Sieh, A. Sladen, H. Hebert, L. Prawirodirdjo, Y. Bock, and J. Galetzka (2007). Coseismic slip and afterslip of the great M_w 9.15 Sumatra–Andaman earthquake of 2004, *Bull. Seismol. Soc. Am.* **97,** S152–S173, doi: 10.1785/0120050631.

DeMets, C., R. G. Gordon, D. F. Argus, and S. Stein (1994). Effect of recent revisions to the geomagnetic reversal time scale on estimation of current plate motions, *Geophys. Res. Lett.* **21,** 2191–2194.

Dziewonski, A. M., T.-A. Chou, and J. H. Woodhouse (1981). Determination of earthquake source parameters from waveform data for studies of global and regional seismicity, *J. Geophys. Res.* **86,** 2825–2852.

Enescu, B., and K. Ito (2001). Some premonitory phenomena of the 1995 Hyogo-ken Nanbu earthquake: Seismicity, *b*-value and fractal dimension, *Tectonophysics* **338,** 297–314.

Engdahl, E. R., A. Villasenor, H. R. DeShon, and C. H. Thurber (2007). Teleseismic relocation and assessment of seismicity (1918–2005) in the region of the 2004 M_w 9.0 Sumatra–Andaman and 2005 M_w 8.6 Nias Island great earthquakes, *Bull. Seismol. Soc. Am.* **97,** S43–S61, doi: 10.1785/0120050614.

Gusman, A. R., Y. Tanioka, T. Kobayashi, H. Latief, and W. Pandoe (2010). Slip distribution of the 2007 Bengkulu earthquake inferred from tsunami waveforms and InSAR data, *J. Geophys. Res.* **115,** no. B12316, doi: 10.1029/2010JB007565.

Habermann, R. E. (1981). Precursory seismicity patterns: Stalking the mature seismic gap, in *Earthquake Prediction: An International Review*, Maurice Ewing Series 4, D. W. Simpson and P. G. Richards (Editors), American Geophysical Union, Washington, D.C., 29–42.

Habermann, R. E. (1987). Man-made changes of seismicity rates, *Bull. Seismol. Soc. Am.* **77,** 141–157.

Hardebeck, J. L., K. R. Felzer, and A. J. Michael (2008). Improved tests reveal that the accelerating moment release hypothesis is statistically insignificant, *J. Geophys. Res.* **113,** no. B08310, doi: 10.1029/2007JB005410.

Heki, K. (2011). Ionospheric electron enhancement preceding the 2011 Tohoku-Oki earthquake, *Geophys. Res. Lett.* **38,** L17312, doi: 10.1029/2011GL047908.

Heki, K., and Y. Enomoto (2013). Preseismic ionospheric electron enhancements revisited, *J. Geophys. Res. Space Phys.* **118,** 6618–6626, doi: 10.1002/jgra.50578.

Imoto, M., and N. Yamamoto (2008). Premonitory changes in seismicity prior to the Great Sumatra–Andaman earthquake of December 26, 2004, *Earth Planets Space* **60,** 693–697.

Kamogawa, M., and Y. Kakinami (2013). Is an ionospheric electron enhancement preceding the 2011 Tohoku-Oki earthquake a precursor? *J. Geophys. Res. Space Phys.* **118,** 1751–1754, doi: 10.1002/jgra.50118.

Kanamori, H. (1981). The nature of seismicity patterns before large earthquakes, in *Earthquake Prediction: An International Review*, Maurice Ewing Series 4, D. W. Simpson and P. G. Richards (Editors), American Geophysical Union, Washington, D.C., 1–19.

Kato, N. (2003). A possible model for large preseismic slip on a deeper extension of a seismic rupture plane, *Earth Planet. Sci. Lett.* **216,** 17–25.

Kato, N., M. Ohtake, and T. Hirasawa (1997). Possible mechanism of precursory seismic quiescence: Regional stress relaxation due to preseismic sliding, *Pure Appl. Geophys.* **150,** 249–267.

Katsumata, K. (2011a). Precursory seismic quiescence before the M_w = 8.3 Tokachi-Oki, Japan earthquake on 26 September 2003 revealed by a re-examined earthquake catalog, *J. Geophys. Res.* **116,** no. B10307, doi: 10.1029/2010JB007964.

Katsumata, K. (2011b). A long-term seismic quiescence started 23 years before the 2011 Off the Pacific Coast of Tohoku earthquake (M = 9.0), *Earth Planets Space* **63,** 709–712.

Katsumata, K., and M. Kasahara (1999). Precursory seismic quiescence before the 1994 Kurile earthquake (M_w = 8.3) revealed by three independent seismic catalogs, *Pure Appl. Geophys.* **155,** 443–470.

Kisslinger, C. (1988). An experiment in earthquake prediction and the 7 May 1986 Andreanof Island earthquake, *Bull. Seismol. Soc. Am.* **78,** 218–229.

Matthews, M. V., and P. A. Reasenberg (1988). Statistical method for investigating quiescence and other temporal seismicity patterns, *Pure Appl. Geophys.* **126,** no. 2/4, 357–372.

Mignan, A., G. King, D. Bowman, R. Lacassin, and R. Dmowska (2006). Seismic activity in the Sumatra–Java region prior to the December 26, 2004 (M_w = 9.0–9.3) and March 28, 2005 (M_w = 8.7) earthquakes, *Earth Planet. Sci. Lett.* **244,** 639–654.

Mogi, K. (1969). Some feature of recent seismic activity in and near Japan (2), Activity before and after great earthquakes, *Bull. Earthq. Res. Inst., Tokyo Univ.* **47,** 395–417.

Nanjo, K. Z., N. Hirata, K. Obara, and K. Kasahara (2012). Decade-scale decrease in *b* value prior to the *M* 9-class 2011 Tohoku and 2004 Sumatra quakes, *Geophys. Res. Lett.* **39,** L20304, doi: 10.1029/2012GL052997.

Ohtake, M. (1980). Earthquake prediction based on the seismic gap with special reference to the 1978 Oaxaca, Mexico earthquake, *Rep. Natl. Res. Cent. Disaster Prev.* **23,** 65–110 (in Japanese).

Ohtake, M., T. Matsumoto, and G. V. Latham (1977). Seismicity gap near Oaxaca, southern Mexico as a probable precursor to a large earthquake, *Pure Appl. Geophys.* **115,** 375–386.

Ohtake, M., T. Matsumoto, and G. V. Latham (1981). Evaluation of the forecast of the 1978 Oacaca, southern Mexico earthquake based on a precursory seismic quiescence, in *Earthquake Prediction: An International Review*, Maurice Ewing Series 4, D. W. Simpson and P. G. Richards (Editors), American Geophysical Union, Washington, D.C., 53–61.

Pesicek, J. D., C. H. Thurber, H. Zhang, H. R. DeShon, and E. R. Engdahl (2010). Teleseismic double-difference relocation of earthquakes along the Sumatra–Andaman subduction zone using a three-dimensional model, *J. Geophys. Res.* **115,** no. B10303, doi: 10.1029/2010JB007443.

Scholz, C. H. (1988). Mechanisms of seismic quiescence, *Pure Appl. Geophys.* **126,** 701–718.

Simoes, M., J. P. Avouac, R. Cattin, and P. Henry (2004). The Sumatra subduction zone: A case for a locked fault zone extending into the mantle, *J. Geophys. Res.* **109,** no. B10402, doi: 10.1029/2003JB002958.

Stuart, W. D. (1979). Strain softening prior to two-dimensional strike slip earthquakes, *J. Geophys. Res.* **84,** 1063–1070.

Tanaka, S. (2010). Tidal triggering of earthquakes precursory to the recent Sumatra megathrust earthquakes of 26 December 2004 (M_w 9.0), 28 March 2005 (M_w 8.6), and 12 September 2007 (M_w 8.5), *Geophys. Res. Lett.* **37,** L02301, doi: 10.1029/2009GL041581.

Tanioka, Y., and A. R. Gusman (2012). Reexamination of occurrence of large tsunamis after the analysis of the 2011 great Tohoku-Oki earthquake (in Japanese), *J. Seismol. Soc. Japan* **64,** 265–270.

Tanioka, Y., Yudhicara, T. Kususose, S. Kathiroli, Y. Nishimura, S. Iwasaki, and K. Satake (2006). Rupture process of the 2004 Sumatra–Andaman earthquake estimated from tsunami waveforms, *Earth Planets Space* **58,** 203–209.

Thomas, J. N., J. J. Love, A. Komjathy, O. P. Verkhoglyadova, M. Butala, and N. Rivera (2012). On the reported ionospheric precursor of the 1999 Hector Mine, California earthquake, *Geophys. Res. Lett.* **39,** L06302, doi: 10.1029/2012GL051022.

Wessel, P., and W. H. F. Smith (1991). Free software helps map and display data, *Eos Trans. AGU* **72,** 445–446.

Wiemer, S. (1996). Analysis of seismicity: New technique and case studies, *Dissertation Thesis*, University of Alaska, Fairbanks, Alaska, 151 pp.

Wiemer, S., and M. Wyss (1994). Seismic quiescence before the Landers (M = 7.5) and Big Bear (M = 6.5) 1992 earthquakes, *Bull. Seismol. Soc. Am.* **84,** 900–916.

Wiemer, S., and M. Wyss (2000). Minimum magnitude of completeness in earthquake catalogs: Examples from Alaska, the western United States, and Japan, *Bull. Seismol. Soc. Am.* **90,** 859–869.

Wyss, M. (1985). Precursors to large earthquakes, *Earthq. Predic. Res.* **3,** 519–543.

Wyss, M., and R. E. Habermann (1988). Precursory seismic quiescence, *Pure Appl. Geophys.* **126,** 319–332.

Wyss, M., and A. H. Martirosyan (1998). Seismic quiescence before the M 7, 1988, Spitak earthquake, Armenia, *Geophys. J. Int.* **134,** 329–340.

Wyss, M., R. E. Habermann, and J.-C. Griesser (1984). Seismic quiescence and asperities in the Tonga–Kermadec Arc, *J. Geophys. Res.* **89,** 9293–9304.

Wyss, M., A. Hasegawa, S. Wiemmer, and N. Umino (1999). Quantitative mapping of precursory seismic quiescence before the 1989, M 7.1 Off-Sanriku earthquake, Japan, *Ann. Geophys.* **42,** 851–869.

Wyss, M., F. W. Klein, and A. C. Johnston (1981). Precursors to the Kalapana M = 7.2 earthquake, *J. Geophys. Res.* **86,** 3881–3900.

Wyss, M., K. Shimazaki, and T. Urabe (1996). Quantitative mapping of a precursory quiescence to the Izu-Oshima 1990 (M = 6.5) earthquake, Japan, *Geophys. J. Int.* **127,** 735–743.

Zhuang, J., Y. Ogata, and D. Vere-Jones (2002). Stochastic declustering of space-time earthquake occurrences, *J. Am. Stat. Assoc.* **97,** 369–380.

Institute of Seismology and Volcanology
Hokkaido University
North-10 West-8, Kita-ku
Sapporo 060-0810, Japan
kkatsu@mail.sci.hokudai.ac.jp

Manuscript received 26 April 2014;
Published Online 6 January 2015